Micelles self-assembled by 3-O-β-D-glucopyranosyl latycodigenin enhances cell membrane permeability, promotes antibiotic pulmonary targeting and improves anti-infect efficacy

Man Zhang
Nankai University
Lili Ye
Nankai University
Hao Huang
Macau University of Science and Technology
Dandan Cheng
Tianjin University of Traditional Chinese Medicine
Wenbo Wu
Nankai University
Kaixin Liu
Nankai University
Zhihong Jiang
Macau University of Science and Technology
Yuanyuan Hou
Nankai University
Gang Bai (gangbai@nankai.edu.cn)
Nankai University College of Pharmacy https://orcid.org/0000-0001-9161-2173

Research

Keywords: 3-O-β-D-glucopyranosyl latycodigenin, self-assembled nanomicelles, cell membrane permeability, lung targeting therapy

Posted Date: May 10th, 2020

DOI: https://doi.org/10.21203/rs.3.rs-27172/v1

Abstract

Background: Nanoparticle-based pulmonary drug delivery systems are commonly developed and applied for drug-targeted delivery. It exhibits significant advantages compared to traditional pulmonary drug delivery systems. However, developing a formulation for each drug is a time-consuming and laborious task.

Results: The present study designed and constructed a universal lung-targeting nanoparticle. The self-assembled micelles were composed of a platycodon secondary saponin, 3-O-β-D-glucopyranosyl platycodigenin 682 (GP-682), via its specific amphiphilic structure. After optimization, the GP-682 micelles obtained a stable zeta potential with a particle size between 60 to 90 nm, and the CMC value was approximately 42.3 μg/mL. Pre-incubation of GP-682 micelles markedly enhanced the cell membrane permeability, and improved drug uptake in vitro . The results were visualized using fluorescent dye tracing, transmission electron microscopy observation and a lactate dehydrogenase releasing assay. The benefits enhanced the distribution of levofloxacin in mouse lung tissue and reduced the overdosing of antibiotic. Pseudomonas aeruginosa PA 14 strain-induced acute lung injury mice model demonstrated that preinjection of GP-682 micelles followed by antibiotic administration produced a higher survival rate and anti-infection efficacy in vivo , which included a reduction in pulmonary injury, bacterial invasion and the expression of cytokines compared to treatment with levofloxacin alone.

Conclusions: GP-682 micelles are another nanoparticle-based pulmonary drug delivery system to increase the use of antibiotic and provide a new option for antibiotic resistance and lung-targeting therapy.

Background

The lungs are a very attractive target for drug delivery because it is generally the end organ of local disease treatment or the route of administration for systemic therapies[1]. It is a suitable portal for many therapeutic interventions because of its large surface area and minimal barriers, which make it easier to gain access into the periphery of the lungs[2]. A pulmonary drug delivery system (PDDS) delivers drugs to the lung to produce a local or systemic therapeutic effect, and it demonstrates unique advantages[3]. Compared with traditional oral administration, the reduced metabolic response of the lung reduces the degradation of the drug, which avoids the first pass effect of the liver[4]. PPDS also improve patient compliance compared to the injection administration[5]. Peptides and other sensitive drugs are suitable for PDDS. Conventional pulmonary dosage forms primarily consist of pressurized metered-dose inhalers (pMDI), dry powder inhalers (DPI) and spray. Traditional pulmonary preparations have some shortcomings, including relatively short duration of action, frequent dosing, and poor patient compliance[6]. Therefore, it is necessary to exploit the new drug delivery system of PDDS to improve the disadvantages of traditional pulmonary preparations.

Nanoparticle-based PPDS developed rapidly, such as polymer nanoparticles, liposomes, solid lipid nanoparticles (SLN), nanostructured lipid carrier (NLC) and micellar system[7]. Previous studies indicated

that nanoparticle-based PDDS improved the uptake and retention of drugs in the lungs and promoted the slow or controlled drug release. For example, mice intravenously injected with liposome-encapsulated ciprofloxacin showed higher levels of drug in sera, lungs, liver and spleen compared to the mice treated with unencapsulated ciprofloxacin, which shows that drug delivery to the infection site was enhanced as a result of the liposome encapsulation of ciprofloxacin[8]. Chitosan is a protein-loaded nanoparticle with low toxicity, biodegradability and mucoadhesive. It is also a representative dosage form of pulmonary route delivery[9]. The encapsulation of drugs in biocompatible and biodegradable excipients, such as liposomes, polymer nanoparticles and micelles, improves the solubility of poorly soluble drugs and prevents the drugs from being devoured by macrophages. Pulmonary administration is affected by a variety of factors, such as particle deposition, lung defense mechanisms, modes of drug administration, drug delivery devices and dosage forms[10, 11]. The existing nanoparticle-based lung delivery systems provide many useful benefits in pulmonary drug administration. However, some challenges must be addressed. The nontargeting of the drug may induce lung inflammation, pulmonary edema and other diseases. The existing nanoparticle-based lung delivery systems were mostly designed and applied for specific diseases and drugs, which makes the drug preparation process too tedious.

Platycodi radix (Jiegeng) is the dried root of *Platycodon grandiflorum* A. DC. (Campanulaceae), and it produces a wide range of pharmacological effects. Jiegeng is widely used to treat respiratory infections, and natural products derived from the roots of Jiegeng regulate the production and secretion of airway mucin, which explains the expectorant and antitussive effects of Jiegeng[12]. More than 100 compounds of saponins, flavones, phenolic acids, polyenes and sterols were identified from Jiegeng[13], the platycosides are considered the key effective ingredients[14]. Modern pharmacological studies showed that platycosides improved cardiovascular system activities and produced neuroprotective, antitumor and antiviral effects[15]. Platycosides also exhibit anti-lipid peroxidation, protect liver fibrosis activities, and promote the recovery of liver damage[16]. It also inhibits microsynthesis to relieve hepatitis[17]. Platycosides have certain effects in regulating obesity, increasing the sensitivity of insulin in diabetic model rats, reducing diabetic vascular complications and regulating the serum index[18, 19]. Platycodin D is a representative platycoside compound that exhibits a wide range of activities, such as antioxidant, anti-tumor and anti-inflammatory[20–22]. Previous studies suggested that platycodins, including deapio-platycodin D (D-PD), deapio-platycodin D3 (D-PD3), platycodin G1 (PG1), platycodin D (PD), platycodin D3 (PD3), and platycodin E (PE), self-assemble in aqueous solutions to form nanomicelles using the dissipative particle dynamics simulations method, which indicates that saponins have great application potential in solubilization[23]. *In vivo* metabolic studies showed that the total saponins of Jiegeng were broken down in the gastrointestinal tract. GP-682 and the platycodon secondary saponin 3-O-b-D-glucopyranosylplatyconic acid 696 (GPA-696) were the main metabolites[24]. GP-682 had better biological activity than GPA-696 in our previous study[25], which helped increase drug delivery to the lung tissue.

The present study designed and prepared the copolymer GP-682, which self-assembled into micelles. The effects of GP-682 micelles on improving cell membrane permeability, increasing cellular uptake, and working as a novel pulmonary drug delivery system, were investigated thoroughly. The newly proposed

nanoparticle-based system was verified in Gram-negative bacteria-induced acute lung injury mice. Pre-injection of GP-682 micelles demonstrated a higher lung tissue distribution of antibiotics. Compared to treatment with antibiotics alone, the anti-infection efficacy improved significantly.

Materials And Methods

Materials

The platycodon secondary saponins (PSS) GP-682 and GPA-696 used in this work were synthesized in our laboratory. N, N-dimethylformamide (DMF) was purchased from Concord Technology Co., Ltd. (Tianjin, China). Nile Red, 9-diethylamino-5H-benzo [alpha] phenoxazine-5-one, was purchased from Aladdin (Beijing, China). FITC was purchased from MedChemexpress (New Jersey, USA). The Cytotoxicity Detection Kit (LDH Activity) was purchased from Roche (Basel, Switzerland). Glutaraldehyde (2.5%) was purchased from GenMed Scientific Inc. (MA, USA). Levofloxacin, one of the broad-spectrum antibiotics of quinolone, and terazosin hydrochloride was purchased from Shanghaiyuanye Bio-Technology Co., Ltd. (Shanghai, China). The *Pseudomonas aeruginosa* PA 14 strain was obtained from associate professor Bai Fang of Nankai University (Tianjin, China). *Pseudomonas aeruginosa* antibody (1001/214) [Alexa Fluor® 488] was purchased from Bio-Techne China Co. Ltd. (Shanghai, China). The concentrations of human IL-6, IL-8 and TNF-α were detected using ELISA kits according to the manufacturer's instructions (Lanpai, Shanghai, China). All cell culture reagents were purchased from Gibco BRL Life Technologies (NY, USA).

Separation and purification of PSS

The PSS of GP-682 and GPA-696 were isolated and purified from a total saponin extract of Radix platycodonis[24]. The preparation process was based on our previously published paper[25]. The purified PSS was identified using HPLC and NMR methods. The detailed data are shown in the Additional file 1 (Fig. S1-S9)

Preparation and characterization of PSS micelles

GP-682 (0.05-4.00 mg) and GPA-696 (0.2 mg) were dissolved in 400 μL of DMF solvent and configured as 0.125 mg/mL to 10 mg/mL solutions. The solution was slowly dropped into 2 mL of pure water under ultrasonic conditions (200 W, SB-25-12DT ultrasonic oscillator, Ningbo Xinzhi Biotechnology Co., Ltd.). After DMF was removed via dialysis against 5X 250 mL water for 12 h, the micelle solution was filtered through a 0.45-μM microporous filter membrane (MCE syringe filter) to obtain a self-assembled micellar solution of PSS. The solution was collected and freeze-dried to obtain the PSS micelles. A Zetasizer (Nano ZS, Malvern Co. Ltd, UK) was used to analyze the particle size, size distribution and the zeta-potential of GP-682 micelles. The morphology of GP-682 micelles was observed using TEM (Talos F200C, FEI, USA).

The stability of GP-682 micelles in the presence of RPMI 1640 with FBS was evaluated using dynamic light scattering (DLS). GP-682 micelles were incubated in RPMI 1640 with 10% FBS at 37 °C for different

time points, then the stability of GP-682 micelles was detected using DLS. Fluorescence spectrophotometry was applied to determine the critical micelle concentration (CMC) value of GP-682 micelles with Nile Red as a probe[26]. GP-682 micelle solutions at concentrations from 0.1 to 1000 μg were prepared. Nile Red (10 μL) in tetrahydrofuran (THF) was added to 1 mL of GP-682 micelle solutions. The final concentration of Nile Red was 10^{-6} mol/L. After sonication for 30 min, the fluorescence emission spectra were measured at 560–700 nm with an excitation wavelength of 550 nm. Emission intensity at 633 nm was plotted against the log of GP-682 concentration.

Cell culture

Human normal lung epithelial cells (BEAS-2B cells) were purchased from American Type Culture Collection (Rockville, MD) and cultured in RPMI medium 1640 containing 10% FBS, 4.5 g/L glucose, L-glutamine and sodium pyruvate. The cells were cultured at 37 °C with 5% CO_2 in a humidified incubator.

Investigation of membrane permeability

BEAS-2B cells were cultured in small confocal dishes. When the cells achieved approximately 80% confluence, different concentrations of GP-682 micelles (0-100 μg/mL) were cocultured with cells for 30 min before 1×10^{-6} mol/L FITC was added. A confocal microscope (Leica TCS SP8) was used to dynamically investigate the entry of FITC into the cells. The excitation wavelength was 488 nm, and the emission wavelength was 600 nm. The cells cultured with GP-682 micelles and FITC were also collected for flow cytometry analysis (BD FACSCalibur System). The excitation wavelength was 490 nm, and the emission wavelength was 530 nm. BEAS-2B cells were also cultured with 100 μg/mL GP-682 micelles for different durations to detect a suitable working time for GP-682 micelles.

Lactate Dehydrogenase (LDH) release assay

BEAS-2B cells were seeded in 200 μL of RPMI 1640 medium with 10% FBS in NUNC 96-well plates. The medium was removed after 48 h, and cells were added with 100 μg/mL GP-682 micelles in RPMI 1640 medium without FBS (serum contains natural LDH activity) for 30 min. The supernatant (100 μL) was collected after these incubations. A mixture of diaphorase/NAD^+ and iodotetrazolium chloride (100 μL) was added to each well. After 1 h at room temperature in the dark, the absorbance was tested at 500 nm (Spark 10M, TECAN, CH).

Morphological observations using TEM

BEAS-2B cells were cultured in a 10-cm cell culture dish. When the cells grew to 80% confluence, GP-682 micelles of 100 μg/mL were added to the cells and cultured at 37 °C for 30 min. BEAS-2B cells without any treatment were used as the control group. The cells were collected and digested with plasma enzymes. Cells were centrifuged at 1000 rpm for 10 min the supernatant was discarded, and cells were washed with precooled normal saline. Cells were centrifuged again, and the supernatant was discarded. The cells were resuspended in 1 mL of 2.5% precooled glutaraldehyde in sodium cacodylate buffer (0.1 M, pH 7.3) as a fixative for 24 h. The cells were desiccated to the critical point and shadowed with platinum. TEM (TecnaiG220, FEI, USA) was used to observe the cells.

Preparation and assay of GP-682/Nile Red micelles

The GP-682/Nile Red micelles were prepared using the same ultrasound method as GP-682 micelle preparation. The proportion of GP-682 to Nile Red was 10:1. Different forms of Nile Red were prepared, including Nile Red dissolved in 0.1% DMSO and GP-682/Nile Red micelles. The final concentration of Nile Red added to cells was identical (1 μg/mL). BEAS-2B cells were cultured in small confocal dishes and divided into three groups: Nile Red group, GP-682/Nile Red micelles group and GP-682 micelles + Nile Red group. In the Nile Red and GP-682/Nile Red micelles groups, the cells were treated with Nile Red or GP-682/Nile Red micelles only. In the GP-682 micelles + Nile Red group, cells were treated with 100 μg/mL GP-682 micelles for 30 min in advance, and the same dose of Nile Red (1 μg/mL) was added. A confocal microscope (Leica TCS SP8) was used to investigate the entry of Nile Red into the cells. The excitation wavelength was 561 nm, and the fluorescence emission spectra were measured at 580–700 nm.

Distribution analysis of lung tissue using HPLC

Ten male Kunming mice (18–22 g) of SPF grade were purchased from Beijing Vital River Laboratory Animal Technology Co., Ltd. After one week of regular rearing, the mice were fasted for 12 h before the experiment. The mice were randomly divided into two groups: the levofloxacin administration group (80 mg/kg), and GP-682 micelles (5 mg/kg) preadministration for 30 min before levofloxacin administration (80 mg/kg) group. The administration method was intraperitoneal injection. The mice were sacrificed at 0.08, 0.25, 0.5, 1.0, 1.5 and 2 h after levofloxacin injection. The lung tissue of the mice was separated after rinsing with normal saline via heart perfusion. One gram of the lung tissue was homogenized with 3 times normal saline buffer. After centrifugation at 3,000 rpm for 10 min, 100 μL of the supernatant was added to 100 μL of an internal standard solution (50 μg/mL terazosin hydrochloride methanol solution) followed by 200 μL of methanol. The solution was mixed thoroughly by vortexing and centrifuged at 10,000 rpm for 15 min. The supernatant (320 μL) was removed and blow-dried with nitrogen. The residue was reconstituted with the addition of 100 μL of methanol and centrifuged at 10,000 rpm for 15 min. The content of levofloxacin in the supernatant was determined using high-performance liquid chromatography (HPLC). The HPLC method was performed in a Shimadzu HPLC (lc-20a) coupled with a fluorescence detector (RF-20A, Shimadzu, Japan). The following chromatographic conditions were used: column, phenomenex Luna C18 (150 mm × 4.6 mm, 5 μm); mobile phase, 10 mmol/L phosphate buffer (containing 0.01% triethylamine, pH 3) - acetonitrile (82:18); flow rate, 1 mL/min; excitation wavelength, 295 nm, emission wavelength, 490 nm; column temperature: 35 °C; and injection volume, 20 μL. Graphpad Prism 8 was used for data processing and analyses. The methodological investigation is detailed in the Additional file 1 (Fig. S10-S11, table 1–3).

Acute lung injury model

Male KM mice (18–22 g) were purchased from Beijing Vital River Laboratory Animal Technology Co., Ltd. Mice were housed under standard specific pathogen-free conditions with 12/12-h light/dark cycles at 23 ± 2 °C and free access to water and food. A total of 105 mice were randomly divided into seven groups (15 mice per group): Model group (Mod); GP-682 micelles group (5 mg/kg GP-682 micelles); levofloxacin

administration groups (Lev-H, 52 mg/kg levofloxacin; Lev-M, 26 mg/kg levofloxacin; Lev-L, 13 mg/kg levofloxacin); and GP-682 micelles preadministration for 30 min groups (GP-682 micelles + Lev-M, 5 mg/kg GP-682 micelles + 26 mg/kg levofloxacin; GP-682 micelles + Lev-L, 5 mg/kg GP-682 micelles + 13 mg/kg levofloxacin). Mice were anesthetized *via* an intraperitoneal injection of a 4% chloral solution (4 μL/g). Activated *P. aeruginosa* PA 14 bacteria (1×10^8/20 μL in PBS) were dropped into the nasal cavity to induce an acute lung infection. The mice were immediately given an antibiotic intervention, except in the Model and GP-682 micelles group. Survival was recorded 6, 8, 10, 12, 14, 16, 18, 20, 22 and 24 h after challenge with the PA-14 bacteria.

Another 48 mice were divided into eight groups, as describe in the survival experiment, except one control group (Con) was added. A mild infection model was used to investigate the effect of combination therapy. Activated PA 14 bacterium was used at 1×10^7/20 μL in PBS for nasal cavity infection. Mice were anesthetized 24 h later via inhalation of ether. Bronchoalveolar lavage (right lung) was performed via the instillation of 1 mL of 0.9% saline through a tracheal cannula, and the fluid was collected for cytokine assays. The left lung tissues of mice were eviscerated and fixed in a formaldehyde solution (10%) for hematoxylin-eosin (H&E) staining and bacterial immunofluorescence detection.

Statistical analysis

The results were reported as the mean values ± SD. Analysis of multiple groups was performed using analysis of variance (One-way ANOVA), and significant differences between two groups were assessed using *t*-tests. The significant differences in survival rate experiment was analyzed by Log-rank text. Differences of $p < 0.05$ were considered statistically significant.

Results And Discussion

Characterization of GP-682 micelles

Structurally, saponins are amphiphilic compounds composed of one or more hydrophilic sugar parts and a lipophilic steroid or triterpenic part. Due to its amphiphilic structure, saponins can self-aggregate and interact specifically with membrane lipids[27]. The amphiphilic GP-682 was identified as a key PSS (shown in Fig. 1a left), which was reported to improve dosimetry of [^{18}F]-phillygenin in lung tissue[25]. The preparations of GP-682 micelles and GP-682/Nile Red micelles were performed using their self-aggregation capacity. The Tyndall phenomenon (shown in Fig. 1a right) suggested that the micelles were formed. The CMC value is a very important parameter of micelles. It involves the self-assembly ability of the amphiphilic copolymer, and it influences the structural stability of micelles *in vitro* and *in vivo*[28]. Therefore, the CMC value of GP-682 micelles was measured using Nile Red as a hydrophobic fluorescence probe. As shown in Fig. 2b, the CMC of GP-682 was approximately 42.3 μg/mL. The relatively low CMC value ensures the stability of GP-682 micelles in the extracellular matrix. The CMC value of saponin also has an important impact on its permeabilizing ability[29]. The relatively low CMC value of GP-682 benefits its permeability of cell membranes compared to other saponins. Unlike

traditional nanomaterials, saponins are safe and effective adjuvants to enhance the absorption of drugs[23]. Therefore, based on the CMC value, the GP-682 micelles should be safe and innocuous compared to other saponins isolated from the roots of Jiegeng, which showed alternative hemolytic effect *in vitro*, especially platycodin D[30].

The zeta potential is also an important index to characterize the stability of colloidal dispersions. The zeta potential of GP-682 micelles in different concentrations were characterized. As shown in Fig. 1c, the zeta potential of most micelles was negatively charged at nearly − 20 mV, except for preparation concentrations less than 0.05 mg/mL. Therefore, the preparation concentration of GP-682 was limited from 0.05 mg/mL to 2 mg/mL in subsequent experiments. The TEM images of GP-682 micelles are exhibited in Fig. 1d. GP-682 micelles prepared between 0.05 to 0.25 mg/mL exhibited a narrow size distribution and appeared spherical with a homogeneous morphology. The optimum size distribution and particle size of GP-682 micelles were characterized between 60 to 90 nm, which is similar to the TEM measurement and suitable for cellular uptake experiments and injection into mice. To detect GP-682 micelle stability in the presence with FBS, the size distribution for different incubation times was detected using DLS. The results demonstrated that the particle size of GP-682 micelles did not change significantly during 24 h (Fig. 1f). These results indicate that the nanoparticles would display *in vivo* stability after injection into mice.

Preincubation of GP-682 micelles improved cellular uptake

The cell membrane is a critical component of the cellular structure, and it protects the cells by separating the cytoplasm from the outside environment. To evaluate the effects GP-682 micelles on membrane permeability, BEAS-2B cells were used for cellular uptake experiments. FITC was selected as a tracer for confocal and flow cytometer observations. As shown in Fig. 2a, after preincubation with GP-682 micelles for 30 min, the cells contained more FITC than untreated cells, and this uptake was dose-dependent. Under the same dose condition, the effect of GP-682 micelles was obviously better than GPA-696 micelles ($p < 0.001$). These results indicated that GP-682 had better structural characteristics and was more suitable as a nanoparticle-based PDDS. When the pretreatment time with GP-682 micelles (100 μg/mL) exceeded 30 min, the cellular uptake of FITC was obviously higher at a relatively stable level (Fig. 2b). Therefore, the best incubation time of GP-682 micelles was selected as 30 min in the next experiments. The flow cytometry experiment demonstrated similar results as the confocal experiment, in which the cells preincubated with GP-682 micelles for 30 min also contained more FITC compared to the untreated cells.

GP-682 micelles induced cell membrane perforation and LDH release

To further verify the effective cell membrane permeability of GP-682 micelles, TEM images were observed in BEAS-2B cells. As shown in Fig. 3a, the membrane surface in control cells was a dense and continuous black line, which demonstrated the integrity of cell membrane. Whole images of cells are shown in

Additional file 1 (Fig. S12). In the 100 μg/mL GP-682 micelles 30 min pretreated group, some pores approximately 60–90 nm were formed on cell membranes, and this size is approximately consistent with the size of the GP-682 micelles. Different from other saponins that induce membrane lysis and lead to the leakage of organelles[31, 32], GP-682 micelles maintained the cell integrity. For example, larger than 1 μM holes in MEL-5 cells were formed after treatment with 10 μM hederacolchiside A1 for 2 min, which induced cell necrosis[33]. The BEAS-2B cells incubated with 100 μg/mL GP-682 micelles for 30 min remained healthy. These images indicated that GP-682 micelles induced membrane perforation without destroying the cells.

LDH, which is often used as a cytosolic marker in the cellular membrane damage test, is a stable cytoplasmic enzyme existing in all cells[33]. BEAS-2B cells were exposed to various concentrations of GP-682 micelles for 30 min at 37 °C. As shown in Fig. 3b, up to the CMC of GP-682 (42.3 μg/mL), the cell contents of LDH were just beginning to release in a concentrate-dependent manner. These results demonstrated that GP-682 micelles changed the permeability of cell membrane to an appropriate degree.

GP-682 micelle preincubation enhanced the efficacy of cellular uptake

Changes in cell membrane permeability are important indicators of drug uptake by cells[34]. Nile Red is an excellent fluorescent lipid probe that is strongly fluorescent only in a lipid environment. When Nile Red is dispersed in an aqueous solution, almost no fluorescence is observed[35]. To investigate the effect of GP-682 micelles on drug entry into cells, two different delivery methods, preincubation with GP-682 micelles or drug directly carried with GP-682 micelles (GP-682/Nile Red micelles), were used to test the cellular uptake effectiveness *in vitro*. The images of Nile Red entering cells and its fluorescence statistics are shown in Fig. 4. Cells in the control group exhibited a slow uptake rate of Nile Red within 20 min of observation. Compared to the control group, the GP-682 micelles group and GP-682/Nile Red micelles group had a faster ingestion speed. The cells pretreated with GP-682 micelles contained more red dye than the cells added with GP-682/Nile Red micelles alone. These data suggest that preincubation with GP-682 micelles achieves higher performance than the GP-682/Nile Red micelles, which have Nile Red wrapped in hydrophobic cavities ($P < 0.05$).

GP-682 micelles changed the distribution of levofloxacin in mice lung

Generally, the high dose of antibiotics contributes to some side effects, such as gastrointestinal reaction, skin allergic reaction and nervous system response[36]. A more serious problem is that long-term use of levofloxacin leads to drug resistance[37]. Therefore, a new strategy to reduce the use of high doses of antibiotics is needed. The active compound of 682 increases drug targeting in mice lung,[25] and GP-682 micelles effectively improved cellular uptake *in vitro*. To evaluate whether GP-682 micelles achieve higher lung tissue uptake *in vivo*, the concentration of levofloxacin in lung tissue was detected using HPLC with or without GP-682 micelle pretreatment for 30 min. As shown in Fig. 4b, the GP-682 micelles combined

levofloxacin group showed a higher level of levofloxacin in lung tissue compared to the levofloxacin group. The AUC_{0-t} of GP-682 micelles combined levofloxacin group was 224.017 ± 34.494, and the AUC_{0-t} of levofloxacin group was 129.796 ± 16.161. Compared with the levofloxacin group, the AUC_{0-t} of GP-682 micelles combined levofloxacin group was 1.8 times of the levofloxacin group. The C_{max} of levofloxacin in GP-682 micelles combined levofloxacin group was increased, and the clearance rate CLz/F was decreased significantly compared to the levofloxacin group. The detailed pharmacokinetic parameters of levofloxacin in mice lung are shown in Additional file 1 (table 4). This result suggests that GP-682 micelles increase the lung delivery of levofloxacin, enhanced levofloxacin utilization, and may promote the antibacterial effect *in vivo*.

GP-682 micelles combination improved antibacterial effects and guaranteed mice survival rate

Levofloxacin could be used to treat *P. aeruginosa*-induced infections in mice[38]. To evaluate the benefits of GP-682 micelles on the adjuvant therapeutic effect, a PA 14 strain of *P. aeruginosa*-induced acute lung infection model was tested in this paper. As shown in Fig. 5a, mice in GP-682 micelles group exhibited the same median survival rate as the model group (14%). This result demonstrated that GP-682 micelles didn't have antibacterial effect. Mice in levofloxacin-treated group showed a higher median survival rate than the model group. However, when low and medium doses of levofloxacin were combined with GP-682 micelles, the survival rate was markedly enhanced compared to the corresponding levofloxacin group ($p < 0.05$).

To detect the anti-infection effect of levofloxacin with or without GP-682 micelles on PA 14-induced mice acute lung injury, the mouse lungs were observed under H&E staining. As shown in Fig. 5b, the lungs of mice in the model group and the GP-682 micelles group exhibited severe bleeding, widened alveolar septa and cell infiltration compared to the control group. Pretreatment with levofloxacin or GP-682 micelles combined with levofloxacin protected the lung from obvious damage. To further test the anti-infection effect, the distribution of PA 14 strains in mouse lung tissue was detected using immunofluorescence staining *via* a fluorescent-labeled Anti-*P. aeruginosa* antibody. As shown in Fig. 5c, the immunofluorescence in the model group and the GP-682 micelles group was significantly stronger than the control group, but the levofloxacin group showed a significant decrease in a dose-dependent manner. The fluorescence in the GP-682 micelles combination group revealed that the low dose of levofloxacin combined with GP-682 micelles showed the same effects as the middle dose of levofloxacin. The middle dose of levofloxacin combined with GP-682 micelles produced the high dose effects of levofloxacin. This result was consistent with the results of H&E staining. Pulmonary perfusates in all groups were also collected to detect inflammation-related factors, including TNF-α, IL-6 and IL-8. The results shown in Fig. 5d, e and f are consistent with the immunofluorescence experiment. These results demonstrated that GP-682 micelles improved the distribution and enhanced lung targeting of levofloxacin.

Previous nanoparticle-based pulmonary drug delivery systems need to encapsulate drugs into the nanomaterials in advance. For example, the antibiotic drug rifampicin, which is used to treat tuberculosis and other pulmonary infections, was encapsulated into porous nanoparticle-aggregate particle to create shelf stability and prolong the action time of rifampicin in lung[39]. Our GP-682 nanomicelle combination with levofloxacin, which could also be used to combine other drugs, provided a more flexible pulmonary drug delivery channel.

Conclusions

In summary, a natural PSS derived from Platycodi radix, GP-682, was used to design and prepare novel self-assembled nanomicelles for application as a PDDS for the first time. Preincubation of GP-682 micelles enhanced the cell membrane permeability and improved drug uptake *in vitro*. The benefits enhanced the distribution of the antibiotic levofloxacin in mouse lung tissue and presented a better anti-infection efficacy *in vivo*. Therefore, combination with the universal nanoparticle-based DDS of GP-682 nanomicelles will provide effective potential in reducing antibiotic resistance and lung-targeting therapy.

Abbreviations

GP-682, 3-O-β-D-glucopyranosyl platycodigenin 682; PDDS, pulmonary drug delivery system; pMDI, pressurized metered-dose inhalers; DPI, dry powder inhalers; SLN, solid lipid nanoparticles; NLC, nanostructured lipid carrier; D-PD, deapio-platycodin D; D-PD3, deapio-platycodin D3; PG1, platycodin G1; PD, platycodin D; PD3, platycodin D3; PE, GPA-696, platycodin E; 3-O-b-D-glucopyranosylplatyconic acid 696; PSS, platycodon secondary saponins; DMF, N, N-dimethylformamide; DLS, dynamic light scattering; CMC, critical micelle concentration; THF, tetrahydrofuran; BEAS-2B cells, Human normal lung epithelial cells; LDH, Lactate Dehydrogenase; HPLC, high-performance liquid chromatography; H&E, hematoxylin-eosin;

Declarations

Ethics approval and consent to participate

All animal care and experimental protocols conformed to the National Institutes of Health guidelines and were approved by the Institutional Animal Care Committee of Nankai University.

Consent for publication

All authors agree to be published.

Availability of data and materials

The datasets supporting the conclusions of this article are included within the article and its Additional file 1.

Competing interests

The authors declare that they have no competing interests.

Funding

This research was supported by International Cooperation and Exchange of the National Natural Science Foundation of China (No. 81761168039), Macau Science and Technology Development 345 Fund (No. 015/2017/AFJ, China).

Author's contributions

1. B. and Y. H. designed the study; M.Z. performed experiments, acquired and analyzed data, drafted and edited the manuscript; L.Y. and D.C. assisted with animal experiments; W.W. and K.L. isolated and purified GP-682; H.H. and Z.J. assisted with experiments. G. B., Y. H., and M.Z. contributed to data discussion and review of the manuscript.

Acknowledgements

Not applicable.

Author's information

[1] State Key Laboratory of Medicinal Chemical Biology, College of Pharmacy and Tianjin Key Laboratory of Molecular Drug Research, Nankai University, Haihe Education Park, 38 Tongyan Road, Tianjin, 300353, People's Republic of China. [2] State Key Laboratory of Quality Research in Chinese Medicine, Macau University of Science and Technology, Taipa, Macau, China. [3] Tianjin University of Traditional Chinese Medicine, Tianjin, 300193, People's Republic of China.

References

1. Courrier HM, Butz N, Vandamme TF. Pulmonary drug delivery systems: recent developments and prospects. Crit Rev Ther Drug Carrier Syst. 2002; 19**:**425-498.
2. Li YZ, Sun X, Gong T, Liu J, Zuo J, Zhang ZR. Inhalable microparticles as carriers for pulmonary delivery of thymopentin-loaded solid lipid nanoparticles. Pharm Res. 2010; 27**:**1977-1986.
3. Sharma ASRMPK. Pulmonary Drug Delivery System: A Novel Approach for Drug Delivery. Current Drug Therapy. 2011; 6**:**14.
4. da Silva PB, de Freitas ES, Bernegossi J, Goncalez ML, Sato MR, Leite CQ, Pavan FR, Chorilli M. Nanotechnology-Based Drug Delivery Systems for Treatment of Tuberculosis–A Review. J Biomed Nanotechnol. 2016; 12**:**241-260.
5. Nakamura K, Akagi S, Ejiri K, Yoshida M, Miyoshi T, Toh N, Nakagawa K, Takaya Y, Matsubara H, Ito H. Current Treatment Strategies and Nanoparticle-Mediated Drug Delivery Systems for Pulmonary

Arterial Hypertension. Int J Mol Sci. 2019; 20.

6. Kuzmov A, Minko T. Nanotechnology approaches for inhalation treatment of lung diseases. J Control Release. 2015; 219:500-518.
7. Yhee JY, Im J, Nho RS. Advanced Therapeutic Strategies for Chronic Lung Disease Using Nanoparticle-Based Drug Delivery. J Clin Med. 2016; 5.
8. Wong JP, Yang H, Blasetti KL, Schnell G, Conley J, Schofield LN. Liposome delivery of ciprofloxacin against intracellular Francisella tularensis infection. J Control Release. 2003; 92:265-273.
9. Lim ST, Forbes B, Martin GP, Brown MB. In vivo and in vitro characterization of novel microparticulates based on hyaluronan and chitosan hydroglutamate. AAPS PharmSciTech. 2001; 2:20.
10. Mangal S, Gao W, Li T, Zhou QT. Pulmonary delivery of nanoparticle chemotherapy for the treatment of lung cancers: challenges and opportunities. Acta Pharmacol Sin. 2017; 38:782-797.
11. Garrastazu Pereira G, Lawson AJ, Buttini F, Sonvico F. Loco-regional administration of nanomedicines for the treatment of lung cancer. Drug Deliv. 2016; 23:2881-2896.
12. Ryu J, Lee HJ, Park SH, Kim J, Lee D, Lee SK, Kim YS, Hong JH, Seok JH, Lee CJ. Effects of the root of Platycodon grandiflorum on airway mucin hypersecretion in vivo and platycodin D(3) and deapi-platycodin on production and secretion of airway mucin in vitro. Phytomedicine. 2014; 21:529-533.
13. Zhang L, Wang Y, Yang D, Zhang C, Zhang N, Li M, Liu Y. Platycodon grandiflorus - an ethnopharmacological, phytochemical and pharmacological review. J Ethnopharmacol. 2015; 164:147-161.
14. Kang SH, Kim TH, Shin KC, Ko YJ, Oh DK. Biotransformation of Food-Derived Saponins, Platycosides, into Deglucosylated Saponins Including Deglucosylated Platycodin D and Their Anti-Inflammatory Activities. J Agric Food Chem. 2019; 67:1470-1477.
15. Nyakudya E, Jeong JH, Lee NK, Jeong YS. Platycosides from the Roots of Platycodon grandiflorum and Their Health Benefits. Prev Nutr Food Sci. 2014; 19:59-68.
16. Kim TW, Lee HK, Song IB, Lim JH, Cho ES, Son HY, Jung JY, Yun HI. Platycodin D attenuates bile duct ligation-induced hepatic injury and fibrosis in mice. Food Chem Toxicol. 2013; 51:364-369.
17. Choi JH, Jin SW, Choi CY, Kim HG, Kim SJ, Lee HS, Chung YC, Kim EJ, Lee YC, Jeong HG. Saponins from the roots of Platycodon grandiflorum ameliorate high fat diet-induced non-alcoholic steatohepatitis. Biomed Pharmacother. 2017; 86:205-212.
18. Zheng J, He J, Ji B, Li Y, Zhang X. Antihyperglycemic effects of Platycodon grandiflorum (Jacq.) A. DC. extract on streptozotocin-induced diabetic mice. Plant Foods Hum Nutr. 2007; 62:7-11.
19. Lee H, Bae S, Kim YS, Yoon Y. WNT/beta-catenin pathway mediates the anti-adipogenic effect of platycodin D, a natural compound found in Platycodon grandiflorum. Life Sci. 2011; 89:388-394.
20. Wang C, Schuller Levis GB, Lee EB, Levis WR, Lee DW, Kim BS, Park SY, Park E. Platycodin D and D3 isolated from the root of Platycodon grandiflorum modulate the production of nitric oxide and secretion of TNF-alpha in activated RAW 264.7 cells. Int Immunopharmacol. 2004; 4:1039-1049.

21. Li W, Tian YH, Liu Y, Wang Z, Tang S, Zhang J, Wang YP. Platycodin D exerts anti-tumor efficacy in H22 tumor-bearing mice via improving immune function and inducing apoptosis. J Toxicol Sci. 2016; 41:417-428.
22. Cho SY, Song CH, Lee JE, Choi SH, Ku SK, Park SJ. Effects of Platycodin D on Reflux Esophagitis due to Modulation of Antioxidant Defense Systems. Evid Based Complement Alternat Med. 2018; 2018:7918034.
23. Dai X, Ding H, Yin Q, Wan G, Shi X, Qiao Y. Dissipative particle dynamics study on self-assembled platycodin structures: the potential biocarriers for drug delivery. J Mol Graph Model. 2015; 57:20-26.
24. Bai ZyTYyHXyHAnLLYTTZJG. Metabolite identification and pharmacokinetic study of platycodi radix (Jiegeng): In vivo. RSC Advances. 2017; 7:7.
25. Shen F, Wu W, Zhang M, Ma X, Cui Q, Tang Z, Huang H, Tong T, Yau L, Jiang Z, et al. Micro-PET Imaging Demonstrates 3-O-beta-D-Glucopyranosyl Platycodigenin as an Effective Metabolite Affects Permeability of Cell Membrane and Improves Dosimetry of [(18)F]-Phillygenin in Lung Tissue. Front Pharmacol. 2019; 10:1020.
26. Shen Y, Zhang Y, Kuehner D, Yang G, Yuan F, Niu L. Ion-responsive behavior of ionic-liquid surfactant aggregates with applications in controlled release and emulsification. Chemphyschem. 2008; 9:2198-2202.
27. Lorent JH, Quetin-Leclercq J, Mingeot-Leclercq MP. The amphiphilic nature of saponins and their effects on artificial and biological membranes and potential consequences for red blood and cancer cells. Org Biomol Chem. 2014; 12:8803-8822.
28. Qiu L, Qiao M, Chen Q, Tian C, Long M, Wang M, Li Z, Hu W, Li G, Cheng L, et al. Enhanced effect of pH-sensitive mixed copolymer micelles for overcoming multidrug resistance of doxorubicin. Biomaterials. 2014; 35:9877-9887.
29. Lorent J, Le Duff CS, Quetin-Leclercq J, Mingeot-Leclercq MP. Induction of highly curved structures in relation to membrane permeabilization and budding by the triterpenoid saponins, alpha- and delta-Hederin. J Biol Chem. 2013; 288:14000-14017.
30. Sun H, Chen L, Wang J, Wang K, Zhou J. Structure-function relationship of the saponins from the roots of Platycodon grandiflorum for hemolytic and adjuvant activity. Int Immunopharmacol. 2011; 11:2047-2056.
31. Kroemer G, El-Deiry WS, Golstein P, Peter ME, Vaux D, Vandenabeele P, Zhivotovsky B, Blagosklonny MV, Malorni W, Knight RA, et al. Classification of cell death: recommendations of the Nomenclature Committee on Cell Death. Cell Death Differ. 2005; 12 Suppl 2:1463-1467.
32. Lemeshko VV, Haridas V, Quijano Perez JC, Gutterman JU. Avicins, natural anticancer saponins, permeabilize mitochondrial membranes. Arch Biochem Biophys. 2006; 454:114-122.
33. Mazzucchelli GD, Cellier NA, Mshviladzade V, Elias R, Shim YH, Touboul D, Quinton L, Brunelle A, Laprevote O, De Pauw EA, De Pauw-Gillet MC. Pores formation on cell membranes by hederacolchiside A1 leads to a rapid release of proteins for cytosolic subproteome analysis. J Proteome Res. 2008; 7:1683-1692.

34. Chen CHQGHZHZMHXYJXJ. Microbubble-Enhanced Cell Membrane Permeability in High Gravity Field. Cellular and Molecular Bioengineering. 2013; 6:12.
35. Fowler SD, Greenspan P. Application of Nile red, a fluorescent hydrophobic probe, for the detection of neutral lipid deposits in tissue sections: comparison with oil red O. J Histochem Cytochem. 1985; 33:833-836.
36. Carbon C. Comparison of side effects of levofloxacin versus other fluoroquinolones. Chemotherapy. 2001; 47 Suppl 3:9-14; discussion 44-18.
37. Trespalacios-Rangel AA, Otero W, Arevalo-Galvis A, Poutou-Pinales RA, Rimbara E, Graham DY. Surveillance of Levofloxacin Resistance in Helicobacter pylori Isolates in Bogota-Colombia (2009-2014). PLoS One. 2016; 11:e0160007.
38. Yagel SK, Barrett JF, Amaratunga DJ, Frosco MB. In vivo oral efficacy of levofloxacin for treatment of systemic Pseudomonas aeruginosa infections in a murine model of septicemia. Antimicrob Agents Chemother. 1996; 40:2894-2897.
39. Sung JC, Padilla DJ, Garcia-Contreras L, Verberkmoes JL, Durbin D, Peloquin CA, Elbert KJ, Hickey AJ, Edwards DA. Formulation and pharmacokinetics of self-assembled rifampicin nanoparticle systems for pulmonary delivery. Pharm Res. 2009; 26:1847-1855.

Figures

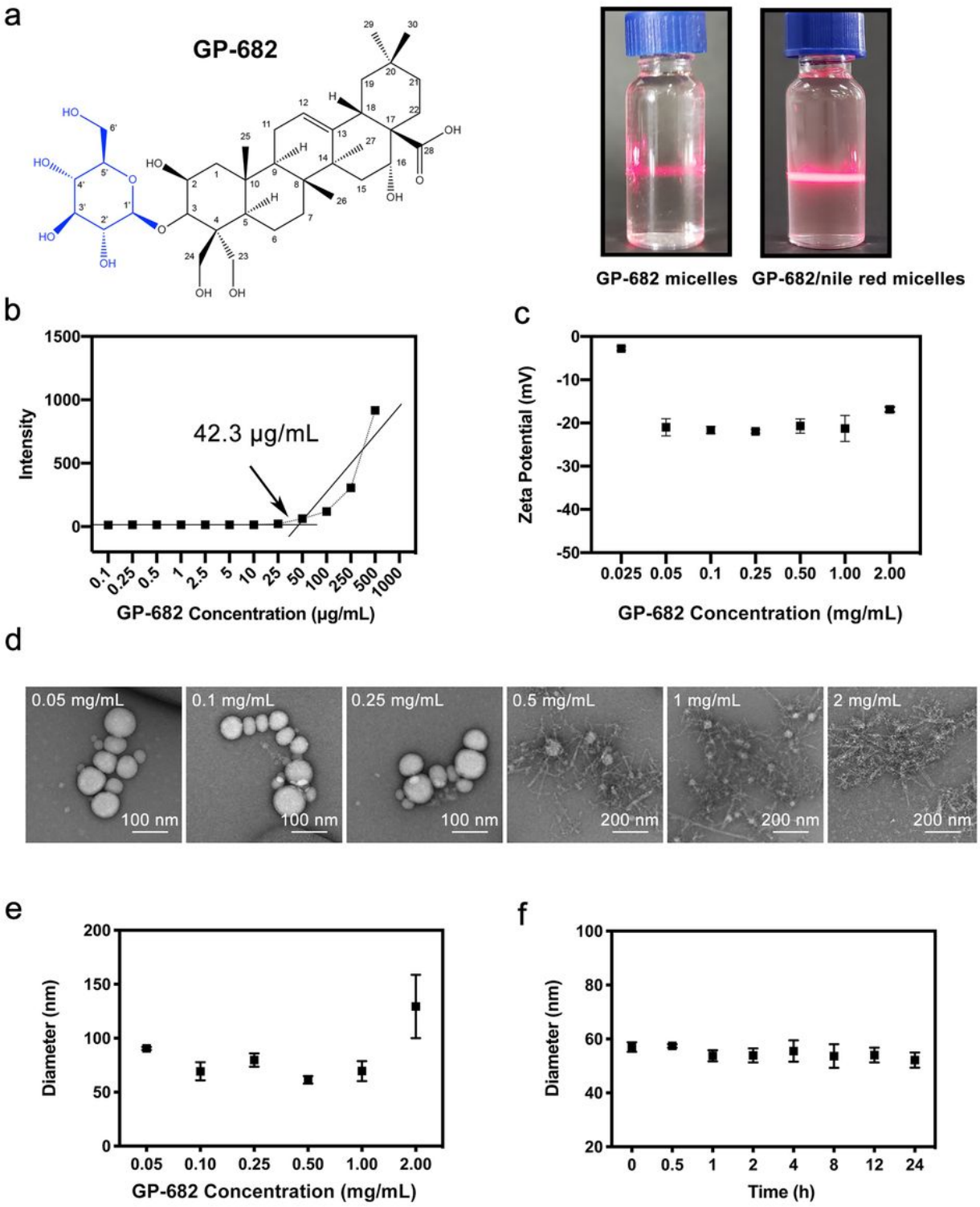

Figure 1

Characterization of GP-682 micelles. (a) The chemical structure of GP-682 and the Tyndall phenomenon of GP-682 micelles and GP-682/Nile Red micelles. (b) The CMC investigation of GP-682. (c) The zeta potential determination of GP-682. (d) The TEM images of GP-682 micelles. (e) The particle size distribution of GP-682 micelles in different concentrations detected using DLS. (f) Stability of mixed GP-682 micelles in the presence of FBS at 37°C. (Data are presented as the means ± SD, n = 3).

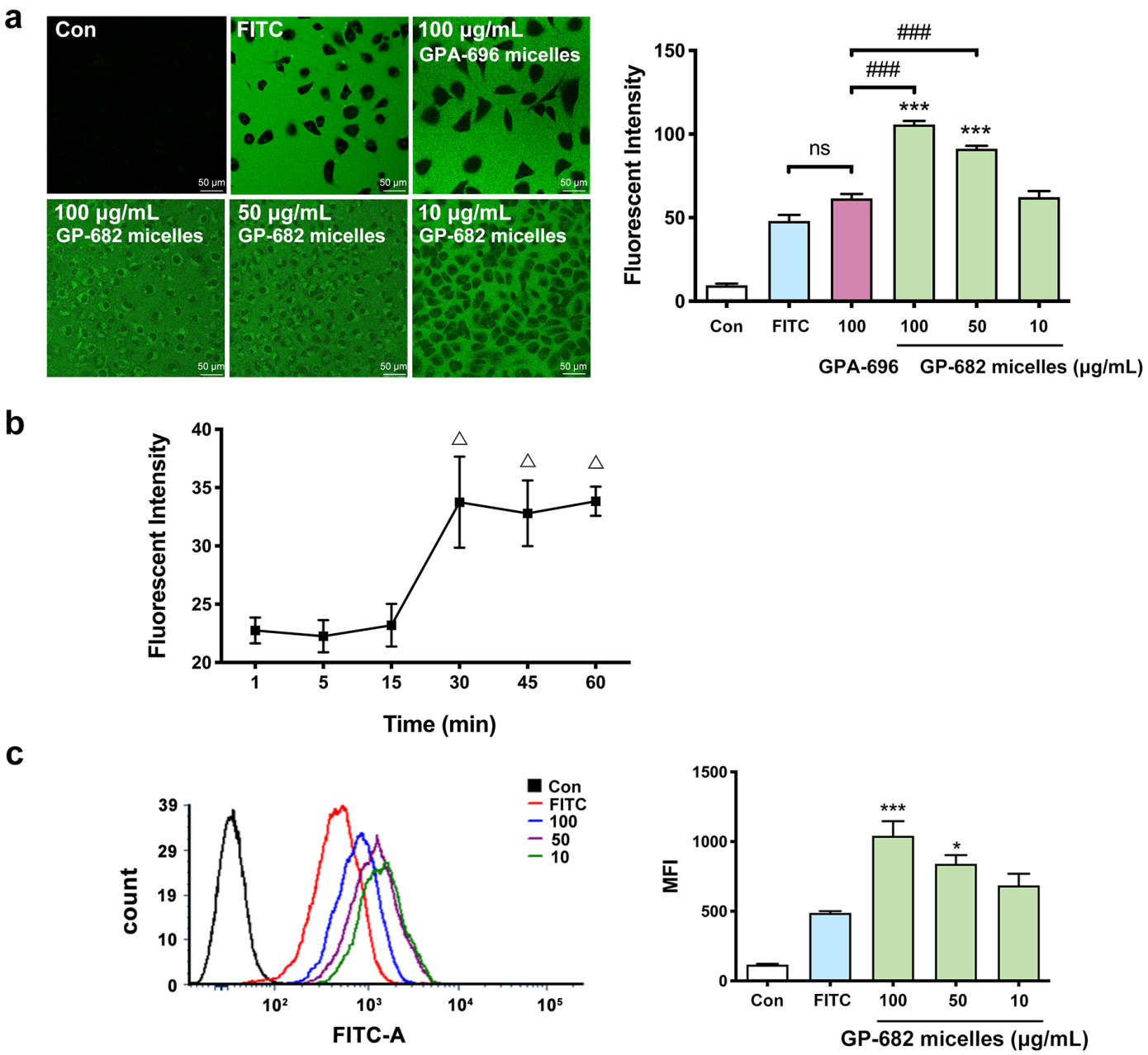

Figure 2

GP-682 micelles enhanced cell membrane permeability in BEAS-2B cells. (a) Fluorescence confocal images of BEAS-2B cell uptake of FITC after 30 min preincubation of different concentrations GP-682 micelles (10, 50, 100 μg/mL) and GPA-696 micelles (100 μg/mL). (b) The investigation of the endocytosis process of BEAS-2B cell uptake of FITC after treatment with 100 μg/ml GP-682 micelles. (c) Flow cytometry intensity assay of BEAS-2B cell uptake of FITC at 30 min after pretreatment with 10, 50, 100 μg/ml GP-682 micelles (left panel). The median florescent intensity (MFI) for each group as summarized in a histogram (right panel). (Data are presented as the means ± SD, n = 3. a, c, *P < 0.05, ***P < 0.001 compared to the FITC group, ###p < 0.001, compared to the 100 μg/mL GPA-696 micelles group; b, △p < 0.05 compared to the cells preincubated with GP-682 micelles for 15 min).

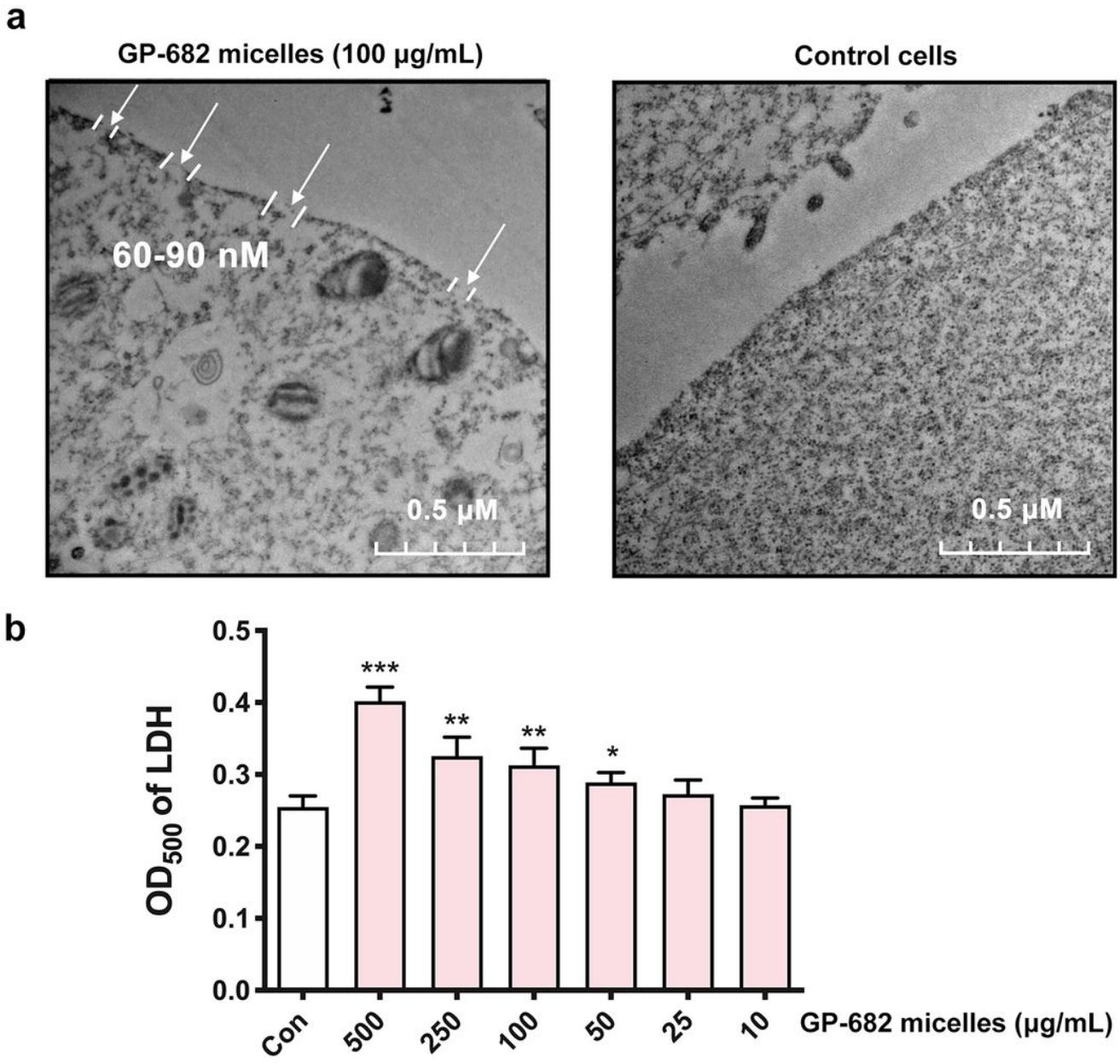

Figure 3

GP-682 micelles changed cell membrane perforation and improved LDH release. (a) Morphological changes in BEAS-2B cells observed using TEM treatment with or without 100 μg/mL GP-682 micelles treatment. (b) The release efficiency for LDH in BEAS-2B cells with 10 to 500 μg/mL GP-682 micelles 30 min treatment. (Data are presented as the means ± SD, n = 3, *p < 0.05, **p < 0.01, ***P < 0.001 compared to the control group).

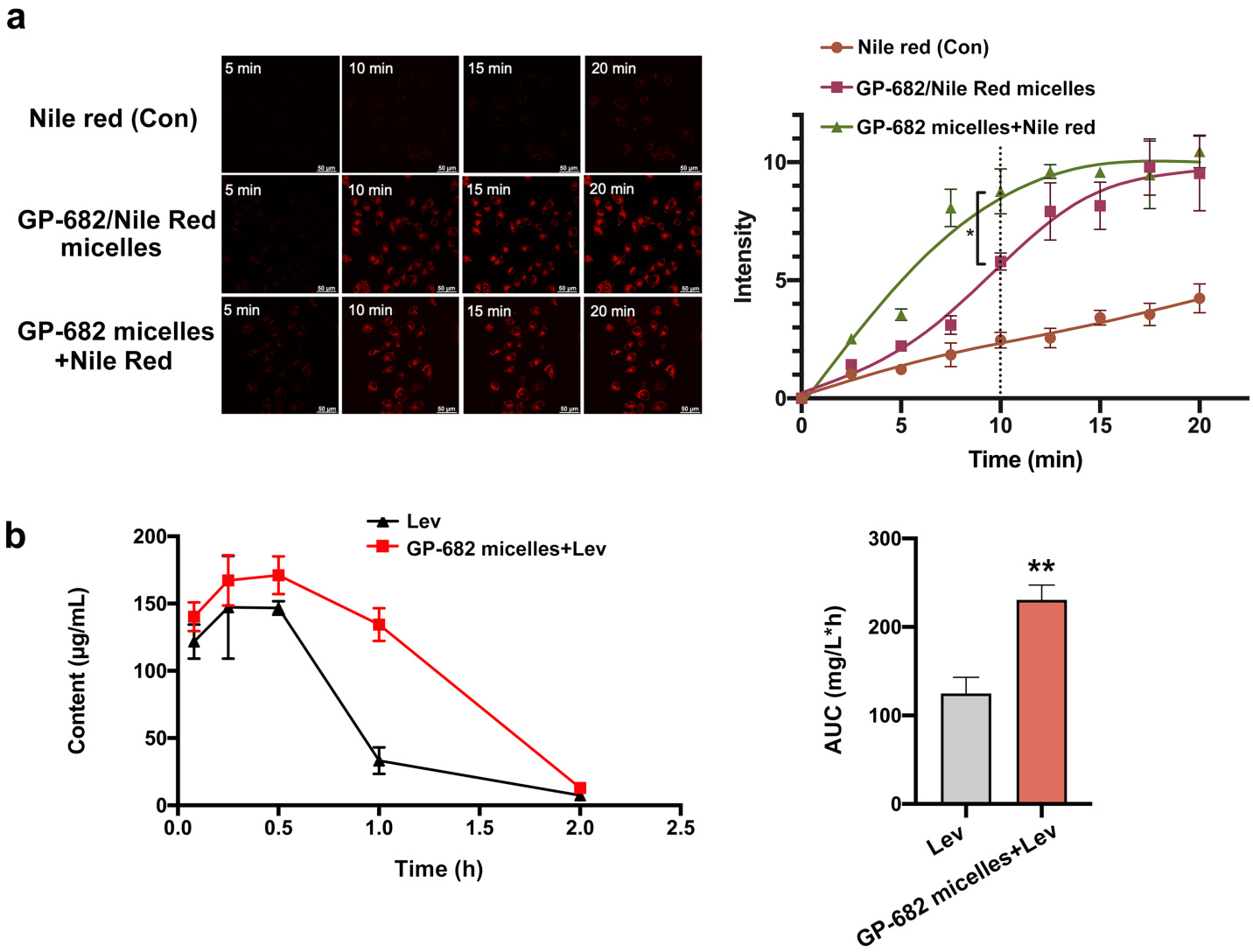

Figure 4

GP-682 micelles enhanced cellular uptake in vitro and improved drug lung targeting in vivo. (a) BEAS-2B cells were treated with Nile Red alone, pretreated with 100 μg/mL GP-682 micelles then Nile Red, or GP-682/Nile Red micelles. Fluorescence of Nile Red was observed using a confocal microscope for 20 min. (Data are presented as the means ± SD, n = 3, *p < 0.05 compared to the GP-682/Nile Red micelles in 10 min). (b) Mice were preinjected with or without GPD-682 micelles (80 mg/kg) for 30 min, then injected with levofloxacin. The pharmacokinetic parameters of levofloxacin in mouse lung tissue was quantified using HPLC. (Data are presented as the means ± SD, n = 5, **p < 0.01 compared to the levofloxacin control group).

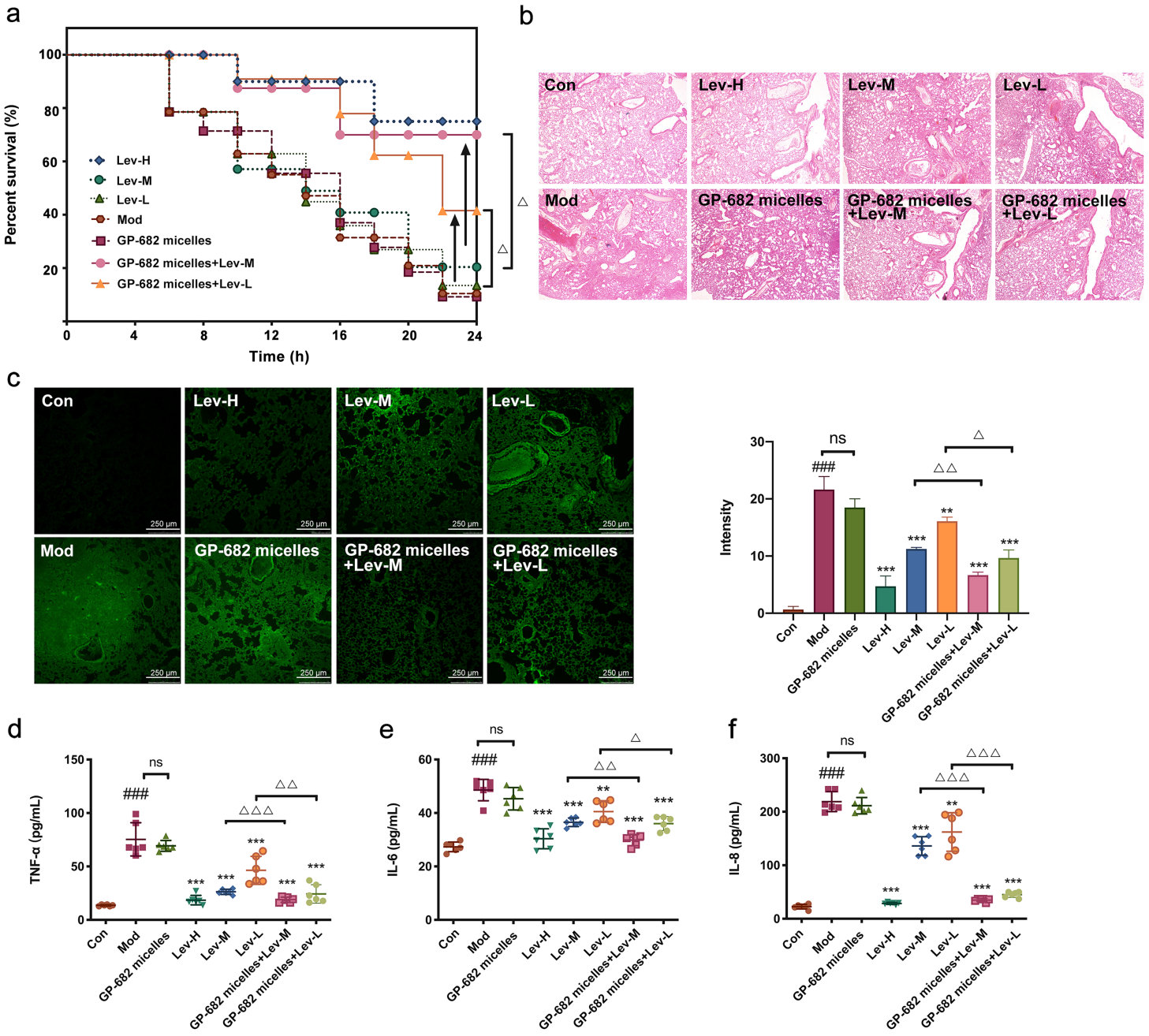

Figure 5

GP-682 micelles improved the antibacterial effect and enhanced mouse survival rate. (a) GP-682 micelles improved mouse survival rate. The KM mice were infected with PA 14 strains followed by intraperitoneal injections of levofloxacin with or without GPD-682 micelles combination. Survival of mice was recorded at 6, 8, 10, 12, 14, 16, 18, 20, 22 and 24 h, respectively, (n = 15); (b) H&E staining images of the mouse lungs (15×). (c) Immunofluorescence images of PA 14 strains distributed in mouse lung.

Supplementary Files

This is a list of supplementary files associated with this preprint. Click to download.

- Additionalfile1.pdf